Journal of Solid State Chemistry **152,** 159–173 (2000)
doi:10.1006/jssc.2000.8679, available online at http://www.idealibrary.com on IDEAL®

New Crystalline Polymers of Ag(TCNQ) and Ag(TCNQF$_4$): Structures and Magnetic Properties

Shannon A. O'Kane,* Rodolphe Clérac,† Hanhua Zhao,* Xiang Ouyang,† José Ramón Galán-Mascarós,† Robert Heintz,* and Kim R. Dunbar†,[1]

†*Department of Chemistry, Texas A&M University, P.O. Box 30012, College Station, Texas 77842-3012, and*
**Department of Chemistry and The Center for Fundamental Materials Research, Michigan State University, East Lansing, Michigan 48824*

Reaction of Ag(BF_4) with [*n*-Bu_4N][TCNQ] in CH_3CN yields a new phase of Ag(TCNQ) referred to as phase I (1). A second polymorph of Ag(TCNQ), denoted phase II (2), which had earlier been prepared by electrocrystallization methods, can be accessed directly from silver powder and neutral TCNQ. The products were characterized by a combination of spectroscopic and physical methods. A powder X-ray diffraction pattern of (1) was indexed as a tetragonal cell with $a = b = 12.1422$ Å, $c = 17.0498$ Å, and $V = 2513.70$ Å^3. Compound (2) crystallizes in the orthorhombic system with $a = 7.2892$ Å, $b = 16.5790$ Å, $c = 17.4448$ Å, and $V = 2108$ Å^3, which correlates well with the lattice parameters $a = 6.975$ Å, $b = 16.686$ Å, $c = 17.455$ Å, and $V = 2031.5$ Å^3 reported for Ag(TCNQ) phase II. Ag(TCNQF$_4$) (5), prepared by electrochemical reduction of $TCNQF_4$ at an Ag electrode, crystallizes in the monoclinic space group $C2/c$, $a = 13.429(3)$ Å, $b = 6.9331(14)$ Å, $c = 25.735(5)$ Å, $\beta = 116.66(3)^\circ$. Ag(TCNQF$_4$) consists of coordinated $TCNQF_4$ radicals arranged in a parallel stacking arrangement along the *b* axis. The nearly "eclipsed" type stacking of the $TCNQF_4$ radicals leads to a short *intra*dimer distance of 3.119(2) Å and an *inter*dimer separation of 3.330(2) Å. Single crystal X-ray data for the salts [Bu_4N][TCNQ] (3) and [*n*-Bu_4N][$TCNQF_4$] (4a) and (4b) are also included for comparison to the Ag(I) materials. [*n*-Bu_4N][TCNQ] (3) crystallizes in the monoclinic space group $P2_1/n$ with $a = 9.3028(7)$ Å, $b = 19.3520(14)$ Å, $c = 15.3880(11)$ Å, $\beta = 100.979\ (2)^\circ$, $V = 2719.6(3)$ Å^3. [*n*-Bu_4N][$TCNQF_4$] crystallizes in two forms; in a monoclinic space group $P2_1/n$ (4a), $a = 7.4244(15)$ Å, $b = 20.212(4)$ Å, $c = 19.758(4)$ Å, $\beta = 97.32(3)^\circ$, $V = 2940.8(10)$ Å^3, and in the triclinic space group $P\bar{1}$ (4b), $a = 9.6335(3)$Å, $b = 14.9574(3)$ Å, $c = 21.3615(5)$ Å, $\alpha = 107.440(1)^\circ$, $\beta = 93.437(2)^\circ$, $\gamma = 104.785(2)^\circ$ and $V = 2808.07(12)$ Å^3. Ring–edge "slipped" stacking arrangements are present in both (4a) and (4b), in which a strongly paired set of $TCNQF_4$ anions interacts with another set. The shortest distance within a dimer pair $TCNQF_4$ in (4a) is 3.09 Å. In contrast, there are two independent types of $TCNQF_4$ interactions in (4b), one that involves strongly interacting anions and one that comprises only weakly dimerized anions. The presence of the latter type in (4b) leads to magnetic properties indicative of thermal population of the triplet excited state at higher temperatures. © 2000 Academic Press

Key Words: **silver; polymers; TCNQ; magnetism.**

INTRODUCTION

The use of transition metal precursors as building blocks in coordination compounds allows for impressive structural diversity and opens up a wealth of potential applications for porous (1), magnetic (2), and conducting (3) solids (1–5). In many cases, knowledge of the geometry of the ligand and the coordination environment of the metal has allowed synthetic chemists to design new strategies and to predict the resulting structural architecture. This concept works well when polymorphism is not an issue, but this is unfortunately not the case with π-stacked charge-transfer materials. Conducting charge transfer materials composed of stacks of donor cations and organic radical acceptors such as those exhibited in Fig. 1 have been under investigation for over 40 years, yet there is still an element of structural serendipity that cannot be denied (3, 5). In addition to classical organic or organometallic donor/acceptor salts that involve π-stacks, polymeric materials composed of a metal ion directly bonded to the organic radical may be envisioned. Such direct bonding between the metal donor and the organic acceptor allows for a combination of the unique characteristics of the transition metal (optical, magnetic, etc.) with the conducting and magnetic properties of organic radical stacks (5a,c–h,j,m–p, 6). A foremost example of this approach is the use of 2,5-DM-DCNQI (Fig. 1b, 2,5-dimethyldicyanoquinodiimine) with Cu (I/II) in the assembly of tetrahedral metal based, three-dimensional networks (3a). The mixed-valent material Cu(DM-DCNQI)$_2$ exhibits an extraordinarily high metallic conductivity (5×10^5 S cm^{-1} at 3.5 K) which is related to the presence of the 1D stacked

[1] To whom correspondence should be addressed. Fax: (979) 845-7177. E-mail: dunbar@mail.chem.tamu.edu.

0022-4596/00 $35.00

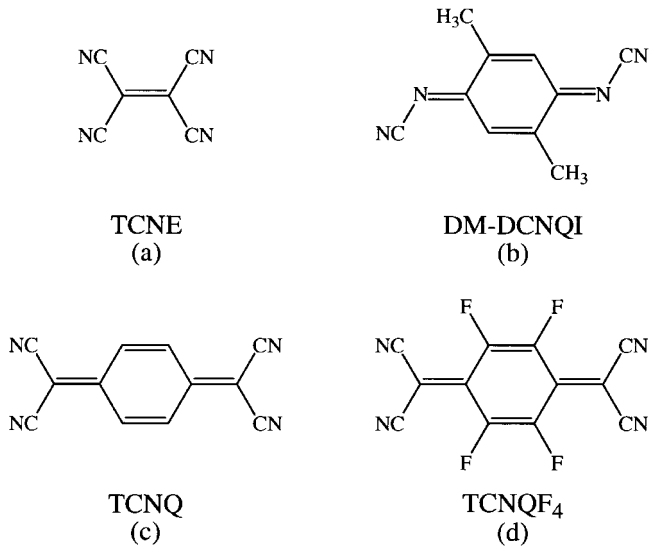

FIG. 1. Organonitrile acceptor molecules used as ligands in metallopolymers.

DCNQI radicals (dicyanoquinodiimine) as well as to interactions of the metal with the ligand via metal d and ligand π orbital overlap. The latter interactions serve to increase the dimensionality of the system and lead to a two-dimensional Fermi surface. The $Cu(DCNQI)_2$ system is an excellent example of how inorganic/organic hybrid materials (3) of the coordination polymer type can be competitive in the area of highly conducting materials.

The incorporation of "bare" metal ions into networks with organic acceptors spawned technological development of binary metal/TCNQ films that behave as switches. Two of the most well-investigated materials in this regard are Cu(TCNQ) ($TCNQ^- = 7,7,8,8$-tetra-cyanoquinodimethanide) and Ag(TCNQ), which exhibit electric-field-induced bistable switching under certain conditions (7, 8). Specifically, the application of an electric field across a thin film of these materials leads to an observable "switching" from a high- to a low-resistance state at a critical threshold potential (8a). For over 20 years there has been intense debate in the literature concerning the mechanism of the switching as well as the role of film growth conditions in dictating the final properties. Earlier this year, our group reported the X-ray structures of two different forms of Cu(TCNQ) with very different magnetic and conducting properties (9). This unrecognized polymorphism in the Cu system has had unfortunate consequences, as it led to many years of fruitless work on mixtures of two compounds. Clearly, further evaluation of other metal/TCNQ and TCNQ derivatives is in order. A search of the literature reveals that the switching behavior of both Cu and Ag devices has been studied, but that the behavior of the Ag(TCNQ) films has not been scrutinized as closely as the Cu(TCNQ) system. In terms of structural evidence, until recently the Ag analog was the better characterized of the two materials. In 1985, Shields reported the single-crystal X-ray structure of a Ag(TCNQ) crystal obtained by electrochemical synthesis (7). No powder data or comments on the singularity of the electrochemical form of Ag(TCNQ) have appeared since this time, however, therefore it is logical to ask if the reported form of Ag(TCNQ) is the only stable phase. In this paper we explore the issue of polymorphism in Ag(TCNQ). In addition, we extended this chemistry to $TCNQF_4$ ($TCNQF_4$: 2,3,5,6-tetrafluoro-7,7,8,8-tetra-cyanoquinodimethanide) (10–12). Although there are several reports of structural (10), magnetic (11), and spectroscopic (12) studies of $TCNQF_4$ charge transfer salts in the literature, the present work constitutes the first structurally characterized metal/$TCNQF_4$ polymer. Analysis of the solid state structure of $Ag(TCNQF_4)$ indicates that it is distinctly different from either phase of Ag(TCNQ) or the alkali metal TCNQ salts (13), but similar to Cu(TCNQ) phase II (9). In addition to results of the Ag(TCNQ) studies, the tetraalkylammonium salts, [*n*-Bu_4N][TCNQ] and [*n*-Bu_4N][$TCNQF_4$], were also subjected to X-ray studies in order to compare the stacking motifs of the TCNQ and $TCNQF_4$ anions in simple organic salts with the pattern found in the Ag polymers.

EXPERIMENTAL

A. Synthesis

Reactions were carried out under a dinitrogen atmosphere unless otherwise indicated. Acetonitrile was dried over 3-Å molecular sieves and distilled under a nitrogen atmosphere prior to use. $Ag(BF_4)$ was purchased from Aldrich Chemical Company, and TCNQ was purchased from TCI Chemical Company and recrystallized from hot acetonitrile. [Bu_4N][TCNQ] (14) and $TCNQF_4$ (15) were prepared according to literature methods, and the $TCNQF_4$ derivatives, Li($TCNQF_4$) and [*n*-Bu_4N][$TCNQF_4$], were prepared in the same way as the TCNQ salts.

(a) Bulk synthesis of Ag(TCNQ) phase I, (**1**). $Ag(BF_4)$ (0.20 g, 1.03 mmol) was dissolved in 20 mL of acetonitrile and filtered through Celite under a nitrogen atmosphere. Separately, [Bu_4N][TCNQ] (0.405 g, 0.906 mmol) was dissolved in 20 mL of acetonitrile and slowly added to the $Ag(BF_4)$ solution. A blue-purple microcrystalline product precipitated immediately, and after 2 min it was collected by filtration, washed with 10 mL of acetonitrile followed by 20 mL of diethyl ether, and dried *in vacuo*; yield 0.254 mg, 90%. Anal. Calcd for $C_{12}H_4N_4Ag$: C, 46.19; H, 1.29; N, 17.95; Found: C, 45.38; H, 1.32; N, 17.51. Characteristic IR data (Nujol mull, KBr plates, cm^{-1}): ν(C≡N), 2199s, 2194sh, 2184s, 2161s; ν(C=C), 1507s; δ(C–H), 824s.

(b) Bulk synthesis of Ag(TCNQ) phase II, (**2**) *from Ag metal.* Ag powder (0.18 g, 1.67 mmol) was suspended in 150 mL of acetonitrile, TCNQ (1 g, 4.89 mmol) was added, and the mixture was stirred in the dark for 2 days. After filtration, the reddish purple microcrystalline product was washed with acetonitrile and suspended in a solution of TCNQ (0.5 g, 2.44 mmol) in 150 mL of acetonitrile to convert any unreacted Ag metal. After 2 additional days of stirring in the dark, the solution was decanted to remove any small particles suspended in the solution. The remaining product was washed thoroughly with acetonitrile, filtered, and dried *in vacuo*; yield 0.45 g, 86.5%. Anal. Calcd for $C_{12}H_4N_4Ag$: C, 46.19; H, 1.29; N, 17.95; Found: C, 45.94; H, 1.38; N, 17.84. Characteristic IR data (Nujol mull, KBr plates, cm^{-1}): ν(C≡N), 2202sh, 2185s, 2170s, 2131sh; ν(C=C), 1505s; δ(C–H), 820s.

(c) Ag(TCNQ) Phase II, (**2**) *from Ag^+ salts.* $Ag(NO_3)$ (0.2 g, 1.18 mmol) was dissolved in 100 mL of acetonitrile, and a solution of [Bu_4N][TCNQ] (0.26 g, 0.58 mmol) in 100 mL of acetonitrile was added dropwise. The mixture was stirred for 5 days, after which time the product was washed thoroughly with acetonitrile, filtered and dried at room temperature. The material was characterized as impure Ag(TCNQ) phase II (**2**) contaminated by a large quantity of Ag metal as determined by X-ray powder diffraction.

(d) Synthesis of [n-Bu$_4$N][TCNQ] (**3**). A quantity of Li(TCNQ) (1.48 g, 0.007 mol) was dissolved in 100 mL of hot distilled water. In a separate flask, an excess of [*n*-Bu_4N]I (5.2 g, 0.0140 mol) was dissolved in 600 mL of boiling distilled water. Upon addition of the Li(TCNQ) solution to the [*n*-Bu_4N]I solution, an instantaneous reaction ensued with the precipitation of a dark purple solid. The solution was stirred and warmed for 1 h, after which time the product was collected by vacuum filtration. The dark purple powder was washed with several aliquots of hot water, followed by diethyl ether, and finally dried *in vacuo*: yield, 3.1 g (99%). The product was recrystallized as follows. The crude product was dissolved in a minimal volume of dichloromethane (~100 mL) and the solution was dried with anhydrous magnesium sulfate. After filtration, the solution was reduced in volume (~30 mL), and an equivalent volume of hexanes was added to induce crystallization. After the excess dichloromethane had been evaporated, the dark purple crystalline product was collected by vacuum filtration, washed with copious amounts of hexanes, and dried *in vacuo*: yield 2.96 g, (95%). Anal. Calcd for $C_{28}H_{36}N_5$: C, 75.29; H, 9.03; N, 15.68; Found: C, 75.66; H, 8.79; N, 15.39. Characteristic IR data (Nujol mull, KBr plates, cm^{-1}): ν(C≡N), 2187 sh, 2181 s, 2160 sh, 2157 s; ν(C=C), 1507 s; δ(C–H), 824 m.

(e) Synthesis of [n-Bu$_4$N][TCNQF$_4$] (**4**). [*n*-Bu_4N]I (1.69 g, 0.458 mmol) was dissolved in 400 mL of hot distilled water. In a separate flask, Li[$TCNQF_4$] (0.650 g, 0.230 mmol) was dissolved in 100 mL of distilled water. Upon the addition of the Li[$TCNQF_4$] solution into the hot solution of [*n*-Bu_4N]I, a dark purple microcrystalline product immediately precipitated. After 1 h of stirring, the product was collected by filtration. The crude product was dissolved in methylene chloride, dried with magnesium sulfate, and the solution filtered. The volume was reduced by evaporation on a rotary evaporator, and 40 mL of hexanes was added to induce precipitation of the product. Crystals of [*n*-Bu_4N][$TCNQF_4$] (**4a**) suitable for X-ray structural determination were obtained directly from this procedure. To recover more product, the methylene chloride was evaporated to produce a second crop of crystals which was collected by filtration, washed with hexanes, and dried *in vacuo*; yield 1.02g, 86%. Anal. Calcd for $C_{28}N_5H_{36}F_4$: C, 64.84; H, 7.00; N, 13.50; Found: C, 64.11; H, 7.63; N, 12.36. Characteristic IR data (Nujol mull, KBr plates, cm^{-1}): ν(C≡N), 2197s, 2174s, 2154s, 2134sh; ν(C=C), 1506 sh, 1498 s.

(f) Bulk synthesis of Ag(TCNQF$_4$) (**5**). $Ag(BF_4)$ (0.135 g, 0.693 mmol) was dissolved in 20 mL of acetonitrile and filtered through Celite, and, separately, [*n*-Bu_4N][$TCNQF_4$] (0.363, 0.70 mmol) was dissolved in 20 mL of acetonitrile. Both solutions were chilled to $-20°C$, and the solution of [*n*-Bu_4N][$TCNQF_4$] was added to $Ag(BF_4)$ and stirred for 2 min. A dark purple-blue, microcrystalline powder was collected by filtration, washed with 10 mL of acetonitrile, 20 mL of diethyl ether, and dried *in vacuo*; yield 0.238g (92%). Anal. Calcd for $C_{12}F_4N_4Ag$: C, 37.53; H, 0.0; N, 14.95; Found: C, 37.12; H, 0.01; N, 14.92. Characteristic IR data (Nujol mull, KBr plates, cm^{-1}): ν(C≡N), 2220s, 2213s, 2197s; ν(C=C), 1501s; ν(C–F), 1208m, 1154w.

B. Structural Studies

A compilation of data collection and refinement parameters for crystals of (**3**)–(**5**) are listed in Table 1.

(*a*) *X-ray structure determination of [n-Bu$_4$n][TCNQ]* (**3**). A typical needle crystal of dimensions $0.21 \times 0.16 \times 0.10\ mm^3$ was mounted on the end of a glass fiber and secured with silicone grease. A hemisphere of data was collected at 173 ± 2 K on a Bruker SMART 1K CCD platform diffractometer (16) with graphite monochromated Mo$K\alpha$ radiation ($\lambda_\alpha = 0.71073$ Å). The frames were integrated in the Bruker SAINT software package (17), and the data were corrected for absorption using the SADABS program (18). Final cell parameters and orientation matrix were obtained from the refinement of XYZ centroids of 3296 reflections with $I > 10\sigma$ with $a = 9.3028(7)$ Å, $b = 19.3520(14)$ Å, $c = 15.3880(11)$ Å, $\beta = 100.979(2)°$, $V = 2719.6(3)$ Å^3. The structure was solved using the SHELXTL V.5.10 package (19) and refinement was carried out by full matrix least-squares calculations on F^2. All the nonhydro-

TABLE 1
Crystallographic Information

	3	4a	4b	5
Formula	$C_{28}H_{40}N_5$	$C_{28}H_{36}F_4N_5$	$C_{28}H_{36}F_4N_5$	$C_{12}F_4N_4Ag$
fw	446.65	518.62	518.62	384.03
T (K)	173(2)	173(2)	173(2)	173(2)
Radiation	Mo $K\alpha$ graphite monochromated ($\lambda_\alpha = 0.71073$ Å)			
Space group	$P2_1/n$	$P2_1/n$	$P\bar{1}$	$C2/c$
a (Å)	9.3028(7)	7.4244(15)	9.6335(3)	13.429(3)
b (Å)	19.3520(14)	20.212(4)	14.9574(3)	6.9331(14)
c (Å)	15.3880(11)	19.758(4)	21.3615(5)	25.735(5)
α (°)	90	90	107.440(1)	90
β (°)	100.979(2)	97.32(3)	93.437(2)	116.66(3)
γ (°)	90	90	104.785(2)	90
V (Å^3)	2719.6(3)	2940.8(10)	2808.07(12)	2141.3(7)
Z	4	4	4	8
d_{calc} (g/cm^3)	1.091	1.171	1.227	2.382
μ (mm^{-1})	0.065	0.088	0.092	1.936
F(000)	972	1100	1100	1464
Total data	16240	35072	13369	6416
Unique data	6327	7113	8918	2526
$R1$ [$I > 2\sigma$][a]	0.0638	0.0507	0.0621	0.0225
$wR2$ [$I > 2\sigma$][b]	0.1111	0.0948	0.1221	0.0586
GOF[c]	0.973	0.997	1.075	1.096

[a] $R1 = \sum [\,\|F_o| - |F_c|\,]/\sum |F_o|$.
[b] $wR2 = \{\sum [w(F_o^2 - F_c^2)^2]/\sum [w(F_o^2)^2]\}^{1/2}$.
[c] GOF $= \{[w(F_o^2 - F_c^2)^2]/(n-p)\}^{1/2}$ where n = total number of reflections and p = total number of parameters.

gen atoms were located and refined anisotropically, and hydrogen atoms were fixed in the idealized positions. The refinement led to final residuals of $R1 = 0.0638$ and a $wR2$ of 0.1111 ($I > 2\sigma$) for all 6327 reflections with 298 parameters with a goodness-of-fit of 0.973. The highest peak in the final difference map was 0.18 e^-/Å^3.

(b) X-ray structure determination of [Bu$_4$N][TCNQF$_4$] (4a). A typical needle crystal of dimension $0.80 \times 0.12 \times 0.10$ mm^3 was mounted on the end of a glass fiber with silicone grease. A full sphere of data was collected at 173 ± 2 K for a [Bu$_4$N][TCNQF$_4$] crystal on a Bruker SMART 1K CCD area detector diffractometer with a graphite monochromated Mo$K\alpha$ radiation ($\lambda_\alpha = 0.71073$ Å). The frames were integrated in the Bruker SAINT software package, and the data were corrected for absorption using the SADABS program. The data were integrated in a $P2_1/n$ monoclinic cell with $a = 7.4244(15)$ Å, $b = 20.212(4)$ Å, $c = 19.758(4)$ Å, and $\beta = 97.32(3)°$. The structure was solved using the SHELXS program (20) and refinement was carried out by full matrix least-squares calculations on F^2 using the SHELXL-97 program (21). All the atoms were refined anisotropically to give final residuals of $R1 = 0.0507$ and a $wR2$ of 0.0946 at a resolution of 0.75 Å. The final refinement was based on 479 parameters and 35,072 reflections, 7113 of which were unique. The highest peak in the final difference map was 0.224 e^-/Å^3.

(c) X-ray structure determination of [n-Bu$_4$N][TCNQF$_4$] (4b). A thin, blue platelet crystal of approximate dimensions $0.20 \times 0.08 \times 0.01$ mm^3 was mounted on a glass fiber and secured with Dow Corning silicone grease. Diffraction data were collected on a Bruker SMART 1K CCD platform diffractometer at 173 ± 2 K. A hemisphere of data was collected at a scan width of 0.3° in ω. Cell parameters were obtained from the refinement of the XYZ centroids of 2850 strong reflections with $I > 10\sigma(I)$ from a total of 15,276 reflections with $a = 9.6335(3)$ Å, $b = 14.9574(3)$ Å, $c = 21.3615(5)$ Å, $\alpha = 107.440(1)°$, $\beta = 93.437(2)°$, $\gamma = 104.785(2)°$, $V = 2808.07(12)$ Å^3. Absorption was corrected for with the program SADABS which led to transmission factors between 0.56 and 1. Data were merged and truncated to 0.85-Å resolution to reduce the high Rsigma. The structure was solved and refined in SHELXTL V. 5.10 package by full-matrix least-squares on F^2. All nonhydrogen atoms were located and refined anisotropically, and hydrogen atoms were fixed in idealized positions. The final refinement was based on 668 parameters and 13,369 reflections, 8918 of which were unique. The refinement led to $R1 = 0.0621$ and $wR2 = 0.1221$ ($I > 2\sigma$). The highest peak in the final difference map was 0.204 e$^-$/Å^3.

(d) X-ray structure determination of Ag(TCNQF$_4$) (5). A typical rectangular platelet crystal of dimensions $0.31 \times 0.16 \times 0.08$ mm^3 was mounted on the end of a glass fiber with silicone grease. A hemisphere of data was collected at 173 ± 2 K for a Ag(TCNQF$_4$) crystal on a Bruker SMART 1K CCD area detector diffractometer with a graphite monochromated Mo$K\alpha$ radiation ($\lambda_\alpha = 0.71073$ Å). The frames were integrated in the Siemens SAINT software package in a $C2/c$ monoclinic cell setting $a = 13.429(3)$ Å, $b = 6.9331(14)$ Å, $c = 25.735(5)$ Å, $\beta = 116.66(3)°$, $V = 2141.3(7)$ Å^3. The data were corrected for absorption using the SADABS program. The structure was solved using the SHELXS program and full matrix least-squares refinement was carried out on F^2 in the SHELXL-97 program. All atoms were refined anisotropically to give final residuals of $R1 = 0.0225$ and $wR2$ of 0.0586 at a resolution of 0.75 Å. The final refinement was based on 191 parameters and 6416 reflections, 2526 of which were unique. The highest peak in the final difference map was 0.811 e^-/Å^3.

C. Physical Measurements

Variable temperature magnetic susceptibility data were obtained in the range 2–300 K on polycrystalline samples using a Quantum Design, Model MPMS-XL and MPMS-5 SQUID magnetometer housed in the Physics and Astronomy Department at Michigan State University. All magnetic data were corrected for the sample holder. The data

TABLE 2
Magnetic Parameters

	$2J$ (K)	χ_{dia} (emu CGS/mol) (value in parenthesis is estimated from the Pascal constants)	χ_{TIP} (emu CGS/mol) (290 K)	C_a (emu CGS.K/mol)	C_b (emu CGS.K/mol)
Ag(TCNQ) phase I (**1**)	—	(-1.0×10^{-4})	0.0013	—	0.0072 (1.9%)
Ag(TCNQ) phase II (**2**)	—	(-1.0×10^{-4})	0.0018	—	0.0009 (0.2%)
Ag(TCNQF$_4$) (**5**)	—	(-1.3×10^{-4})	0.0010	—	0.0082 (2.2%)
[Bu$_4$N] [TCNQ] (**3**)	> 2000	-3.0×10^{-4} (-2.9×10^{-4})	— —	— —	0.0004 (0.1%)
[Bu$_4$N][TCNQF$_4$] (**4a**)	—	-3.8×10^{-4} (-3.2×10^{-4})	—	—	0.0006 (0.2%)
[Bu$_4$N][TCNQF$_4$] (**4b**)	158	-3.7×10^{-4} (3.2×10^{-4})	—	0.75	0.0021 (0.6%)

Note. C_a is the Curie constant from the Bleaney–Bowers fitting, C_b is the Curie constant of the impurity, which is 0.375 for one spin $S = 1/2$, and the percentage of impurity is in parenthesis.

for Ag(TCNQ) and Ag(TCNQF$_4$) were corrected for diamagnetism from Pascal constants (22), -1×10^{-4} and -1.3×10^{-4} emu CGS/mol, respectively. Key results of the magnetic studies are listed in Table 2. Infrared spectra were recorded on solids suspended in Nujol on KBr plates using a Nicolet IR/42 FT-IR spectrometer. Field emission scanning electron microscopy (FESEM) measurements were performed on a Hitachi Ltd., Model S-4700II with a tungsten filament housed in the W. M. Keck Microfabrication Facility located in the Department of Physics and Astronomy at Michigan State University.

RESULTS AND DISCUSSION

The controversy (8) over the purported bistable switching phenomenon of Cu(TCNQ) films (8a) along with our recent verification of two distinct phases of Cu(TCNQ) (9), prompted us to investigate related metal/TCNQ systems. Reports of switching behavior for devices containing Ag and other organic acceptors (8b,g,n) such as TCNQF$_4$, 2,5-dimethoxy-7,7,8,8-tetracyanoquinodimethane (TCNQ(OMe)$_2$), 11,11,12,12-tetracyano-2,6-napthoquino-dimethane (TNAP), and tetracyanoethylene (TCNE) point to this metal as a logical choice for further synthetic and structural studies. To date, single crystal X-ray data have been published for only one phase of Ag(TCNQ) (**2**) as obtained from electrochemical methods (8). Since the stoichiometry of Ag(TCNQ) is identical to that of Cu(TCNQ), namely 1:1, it seemed a likely prospect to exhibit more than one polymorph as well. Along with this issue, it was of interest to study the corresponding perfluorinated TCNQ derivative, TCNQF$_4$, to probe if electronic changes in the organic acceptor influences the stability of various phases.

A. Synthesis of Bulk Phases

The two main aims of this study were (i) to determine whether a second Ag(TCNQ) polymorph exists and (ii) to obtain pure samples of the materials for physical properties measurements. In accord with the literature methods, we have verified that one type of crystalline Ag(TCNQ) (phase II) can be prepared in bulk by the direct reaction of Ag metal with TCNQ:

$$\text{Ag(s)} + \text{TCNQ} \xrightarrow{\text{MeCN}} \text{Ag(TCNQ) phase II.} \qquad [1]$$

Another route is the simple metathesis reaction shown in Eq. [2], which is advantageous for several reasons: the metal and ligand are in the desired oxidation states, the reagents are completely soluble, and the product precipitates upon formation which allows it to be separated from by-products. Furthermore, this reaction leads to essentially quantitative yields:

$$\text{Ag(BF}_4) + [n\text{-Bu}_4\text{N}]\,[\text{TCNQ}] \xrightarrow{\text{MeCN}} \text{Ag(TCNQ) phase I} + [n\text{-Bu}_4\text{N}]\,[\text{BF}_4]. \qquad [2]$$

Variations in reaction times and temperatures do not significantly alter the outcome of the reaction in Eq. [2]. The stable product is a previously unrecognized phase of Ag(TCNQ), which we refer to as phase I (**1**). Obviously the relationship between the two Ag(TCNQ) phases is not simply a matter of kinetic versus thermodynamic products, as in the case of Cu(TCNQ) phases I and II. Attempts to convert Ag(TCNQ) phase I to phase II were not very successful and led to a mixture of phases. These experiments

were performed on the basis of the idea that these materials would be related to each as found for Cu(TCNQ). Simply put, we thought that phase I was a kinetic product that would convert to the thermodynamic product, phase II, upon heating in solution. There is no evidence that this is the case for Ag(TCNQ), and it appears that phase I which is only slightly soluble does not readily convert to phase II, except by formation of silver metal and neutral TCNQ. This conclusion is based on the observation that suspensions of Ag(TCNQ) phase I in CH_3CN that are not heated and protected from light do not show any conversion to phase II. On the other hand, if the solutions are warmed and exposed to light, phase II and Ag metal are formed as judged by powder X-ray methods. In light of these findings, it is not possible to cite either of the phases as being the kinetic or thermodynamic product. It may be that low solubility prevents the conversion of phase I to phase II, or it may simply be that phase II can only be formed by the direct reaction of Ag metal and TCNQ.

$Ag(TCNQF_4)$ is prepared similarly to phase I of Ag(TCNQ) (Eq. [3]). Analysis of the solid-state structure of $Ag(TCNQF_4)$ (**4**) indicates that it is distinctly different from either phase of Ag(TCNQ), and, interestingly, it appears to be the only phase. Reaction conditions were varied in a similar manner to what was performed with Ag(TCNQ), but all reactions yielded the same crystalline material as judged by powder X-ray methods.

$$Ag(BF_4) + [n\text{-}Bu_4N][TCNQF_4] \xrightarrow{MeCN} Ag(TCNQF_4) + [n\text{-}Bu_4N][BF_4]. \quad [3]$$

B. Infrared Spectroscopy

Infrared spectroscopy is a useful technique for characterizing TCNQ charge transfer salts, especially with respect to distinguishing the presence of TCNQ in its neutral versus reduced forms (5f, 23). As expected, IR spectra of both Ag(TCNQ) phases are similar due to their structural similarities and their basic formulation as compounds of $TCNQ^-$. Table 3 summarizes the pertinent data for compounds (**1–5**). In the $\nu(C\equiv N)$ region, several stretching frequencies indicate the presence of $TCNQ^-$. Ag(TCNQ) phase I exhibits strong, broad absorptions at 2199, 2194, 2184, and 2161 cm^{-1}, while Ag(TCNQ) phase II shows a similar pattern at slightly lower frequencies, viz., 2202, 2185, 2170, 2131 cm^{-1}. These modes are lower in energy than the $\nu(C\equiv N)$ stretch of neutral TCNQ, which occurs at 2222 cm^{-1}, and are characteristic of $TCNQ^-$. $Ag(TCNQF_4)$ exhibits strong absorptions at 2220, 2213, and 2197 cm^{-1} in accord with data for salts containing $TCNQF_4^-$ (24). Neutral $TCNQF_4$ occurs at 2225 cm^{-1} (15). The $\nu(C=C)$ stretching region is characteristic for the TCNQ and $TCNQF_4$ phenyl rings. The π-bond delocalization over the ring results in one strong (C=C) stretch ranging from 1500 to 1510 cm^{-1} for $TCNQ^-$. Ag(TCNQ) phases (I and II) and $Ag(TCNQF_4)$ spectra exhibit $\pi(C=C)$ features at 1507, 1505, and 1501 cm^{-1}, respectively. The δ(C–H) bending mode is also a sensitive indicator of the presence of $TCNQ^-$, $TCNQ^{2-}$, and mixed-valence stacks of $TCNQ^-$/TCNQ (25). Ag(TCNQ) phases I exhibits a weak absorption at 824 cm^{-1}, while phase II exhibits a lower energy mode at 820 cm^{-1}. Both frequencies are within the range reported for reduced TCNQ.

TABLE 3
Experimental IR Data for 1–5 and Selected Reference Compounds

	IR			
	ν (C≡N) (cm^{-1})	ν (C=C) (cm^{-1})	δ (C–H) (cm^{-1})	Refs.
Cu(TCNQ)				
Phase I	2199 s, br; 2172 s		825 s	9
Phase II	2211 s, 2172 s		825 s	9
Ag(TCNQ)				
Phase I (**1**)	2199 s, 2194 sh, 2184 s, 2161 s	1507 s	824 s	
Phase II (**2**)	2202 sh, 2185 s, 2170 s, 2131 sh	1505 s	820 s	
$Ag(TCNQF_4)$ (**5**)	2220 s, 2213 s, 2197 s	1501 s		
$[n\text{-}Bu_4N][TCNQ]$ (**3**)	2188 sh, 2180 s,	1507 s	824 s	
TCNO	2222 s	1541 s	861 s	15 c
$[n\text{-}Bu_4N][TCNQF_4]$ **4a**	2197 s, 2178 s	1499 ms		
$[n\text{-}Bu_4N][TCNQF_4]$ **4b**	2194 s, 2174 s,	1499 ms		
$TCNQF_4$	2259 br, 2225 s, 2211 s	1489 s		15 b, 12 e

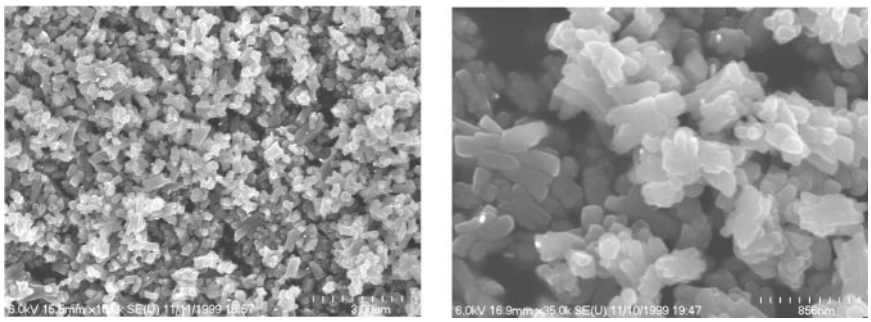

FIG. 2. FESEM photographs of Ag(TCNQ) phase I (**1**) at various magnifications.

C. Structural and Magnetic Studies

A determination of the solid-state structures of metal/TCNQ switching materials is crucial to fully understanding their unusual behavior. Despite several attempts to obtain single crystals of Ag(TCNQ) phase I (**1**), small crystal size and/or twinning prevented a single crystal analysis. X-ray powder diffraction, however, was very useful for discerning the differences between phase I and phase II. X-ray quality crystals of Ag(TCNQF$_4$) (**5**) and the starting materials, [*n*-Bu$_4$N][TCNQ] (**3**) and [*n*-Bu$_4$N][TCNQF$_4$] (**4a**) and (**4b**), were isolated and their structural and magnetic data are presented here.

(*a*) *Field Emission Scanning Electron Microscopy (FESEM) Studies*

The use of high-resolution microscopy was very useful for discerning morphological differences in the two phases of Cu(TCNQ) (9). FESEM images of Ag(TCNQ) phase I and II shown in Figs. 2 and 3, respectively indicate that both exhibit needle-like morphologies, although it is clear that phase II is much more crystalline. Images of single crystals of Ag(TCNQF$_4$) and [*n*-Bu$_4$N][TCNQF$_4$] are provided in Fig. 4. The single crystal of Ag(TCNQF$_4$) is a representative size for those obtained through electrocrystallization, while the crystal of [*n*-Bu$_4$N][TCNQF$_4$] is typical of samples obtained in the bulk synthesis.

(*b*) *Powder X-Ray Diffraction of Solution Prepared Phases*

X-ray powder diffraction methods were used to distinguish the two phases of Ag(TCNQ). Although the crystal structure of phase II is known, it is important to compare both bulk products with the reported crystal structure. Figure 5 displays powder diffraction patterns of bulk samples of phases I and II (Figs. 5a and 5b) and a simulated pattern (Fig. 5c) from the X-ray data of Ag(TCNQ) phase II. Samples were analyzed using a step program (12 s per 0.02° at 2Θ) on a Rigaku RU200B X-ray powder diffractometer with Cu$K\alpha$ radiation ($\lambda_\alpha = 1.54050$ Å). The experimental patterns were indexed using the Treor 90 program (26). This led to the tetragonal cell with $a = b = 12.1422$ Å, $c = 17.0498$ Å, and $V = 2513.70$ Å^3 for Ag(TCNQ) phase I and an orthorhombic cell with $a = 7.2892$ Å, $b = 16.5790$ Å, $c = 17.4448$ Å, and $V = 2108$ Å^3 for the bulk Ag(TCNQ) phase II product. The indexed parameters for Ag(TCNQ) phase II are comparable to the lattice parameters published (7) for the Ag(TCNQ) crystal ($a = 6.975$ Å, $b = 16.686$ Å, $c = 17.455$ Å, and $V = 2031.5$ Å^3). Figure 5d is a hypothetical powder pattern simulated from the experimental powder

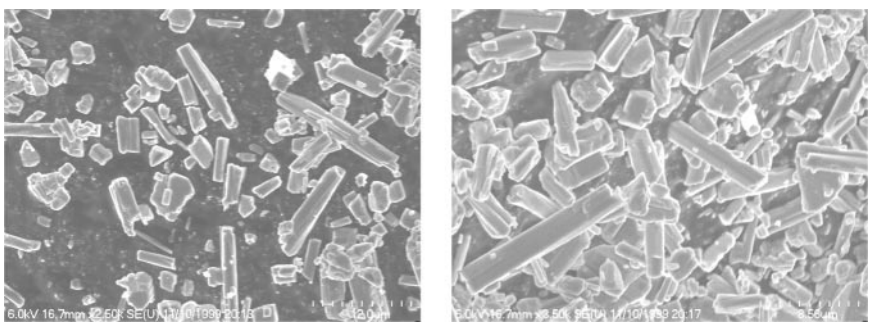

FIG. 3. FESEM photographs of Ag(TCNQ) phase II (**2**) at various magnifications.

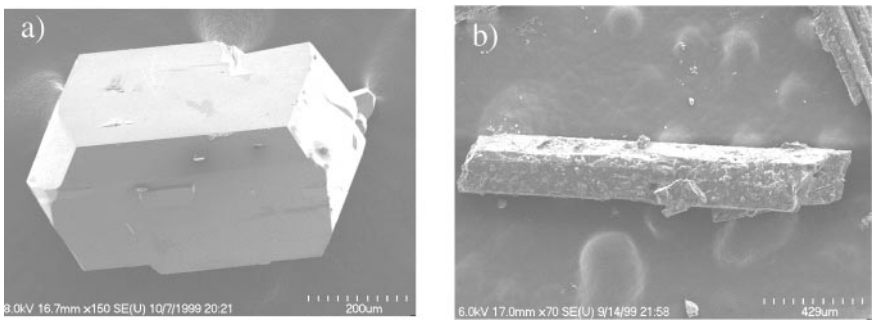

FIG. 4. FESEM photographs of (a) $Ag(TCNQF_4)$ (**5**) and (b) [*n*-Bu_4N][$TCNQF_4$] (**4a**) at various magnifications.

pattern of Phase II. This was accomplished by raising the symmetry of cell for phase II from orthorhombic to tetragonal. This exercise was undertaken to further support our contention that phase I is tetragonal and that it bears a strong structural relationship to crystallographically determined phase II.

A comparison of the experimental powder pattern for a bulk sample of $Ag(TCNQF_4)$ and a simulated pattern from the single crystal X-ray data are depicted in Fig. 6 from which it is obvious that the structures of the samples are identical.

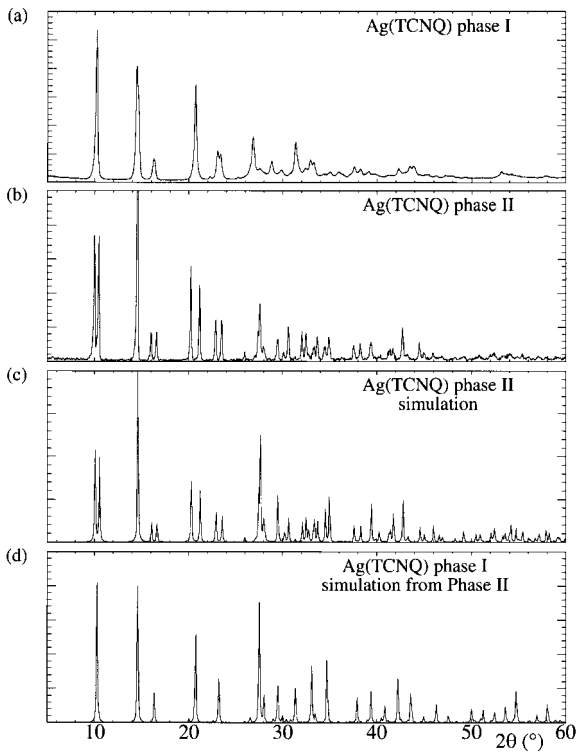

FIG. 5. Experimental powder X-ray diffraction patterns for (a) Ag(TCNQ) phase I (**1**), (b) Ag(TCNQ) phase II (**2**) and simulated powder X-ray diffraction patterns for (c) Ag(TCNQ) phase II (**2**), (d) Ag(TCNQ) phase I (**1**).

(*c) Single Crystal Diffraction Studies and Magnetic Measurements*

(i) Single crystal growth. X-ray quality crystals of [*n*-Bu_4N][TCNQ] (**3**) and [*n*-Bu_4N][$TCNQF_4$] (**4a**) were both obtained from treatment of the reaction solutions with hexanes, whereas [*n*-Bu_4N][$TCNQF_4$] (**4b**) was obtained from the slow diffusion of water into a methanol solution of [*n*-Bu_4N][$TCNQF_4$] (**4a**). Crystals of $Ag(TCNQF_4)$ (**5**) were obtained by electrocrystallization methods similar to those employed by Shields to prepare crystals of Ag(TCNQ) phase II (**2**). Electrochemical reduction of $TCNQF_4$ was carried out at room temperature by slow reduction of TCNQ at a Ag electrode (1 mm in diameter and 15 mm long) in a two-compartment electrolysis cell filled with 20 mL of acetonitrile. The largest crystals were obtained with 15 mg of $TCNQF_4$ and a constant current of 3 μA. The light yellow solution slowly turned dark green with concomitant deposition of crystals on the silver electrode. After a period of 2 weeks (corresponding to the consumption of 80% of the $TCNQF_4$), crystals were collected, washed with acetonitrile, and dried *in vacuo*.

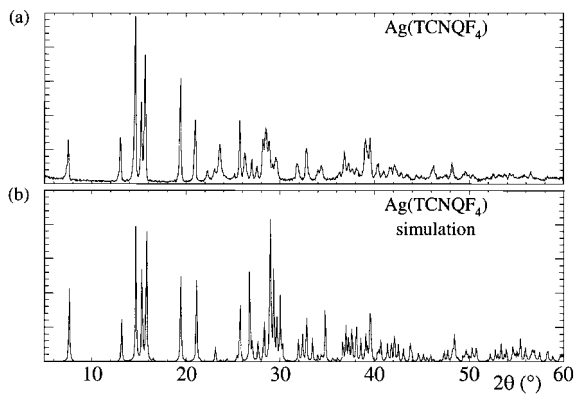

FIG. 6. (a) Experimental and (b) simulated powder X-ray diffraction patterns for $Ag(TCNQF_4)$ (**5**).

(*ii*) [*n*-Bu$_4$*N*][*TCNQ*] (**3**). In this salt, two TCNQ anion radicals are related by an inversion center, and form a completely isolated dimer $(TCNQ)_2^{2-}$, which is stacked in a nearly eclipsed pattern in the ring-ring mode (Fig. 7). Refinement of the least-squares plane of the dimer revealed the interplanar distance of the dimer to be 3.218(2) Å, which is shorter than the sum of the van de Waals radii between carbon atoms of aromatic rings (3.4 Å) (27). This strong dimerization leads to a diamagnetic ground state as clearly evident from the plot in Fig. 8. The diamagnetic value estimated from the Pascal constants (22) at -2.9×10^{-4} emu CGS/mol is in good agreement with the experimental value obtained -3.01×10^{-4} emu CGS/mol. Above 260 K, a small increase in the susceptibility can be detected, which is a signature of the thermal population of the triplet state with an energy gap greater than 2000 K.

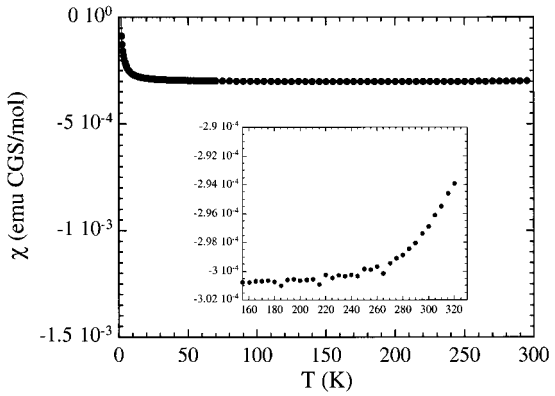

FIG. 8. Temperature dependence of the magnetic susceptibility for [*n*-Bu$_4$N][TCNQ] (**3**). The high-temperature region emphasizing the population of the triplet state is shown as an insert.

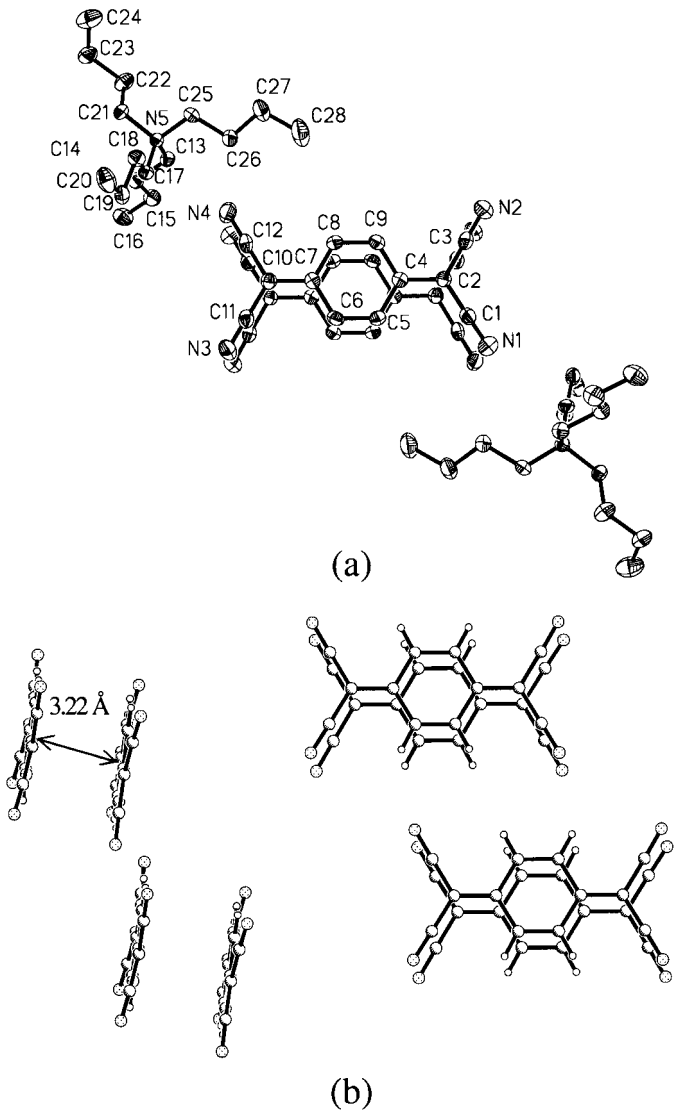

FIG. 7. (a) ORTEP drawing (at the 50% probability level) and (b) packing arrangement of the TCNQ anions in [*n*-Bu$_4$N][TCNQ] (**3**).

(*iii*) [*n-Bu$_4$N*][*TCNQF$_4$*] (**4a** *and* **4b**). In (**4a**), the $TCNQF_4^-$ radicals form a strongly dimerized chain with two interplanar distances of 3.088(4) and 3.349(4) Å (Fig. 9). The *intra*dimer distance is shorter than those reported for other simple TCNQ salts (27). With this type of ring–edge dimer structure (Fig. 9b), with its short intermolecular distance, the compound is rigorously diamagnetic over the entire temperature range. The susceptibility is -3.8×10^{-4} emu CGS/mol which is close to the value calculated from the Pascal constants, viz., -3.2×10^{-4} emu CGS/mol.

In (**4b**), there are two independent $TCNQF_4$ anions in the asymmetric unit, which are involved in two different types of dimer pairs. These two sets of radicals are oriented with an angle between the least-square planes of about 70°. The first set of dimers (Figs. 10b and 10c) exhibits a nearly eclipsed ring–ring type pattern related by an inversion center and with a stacking distance of 3.206(5) Å. These dimers form a chain along the a axis at an *inter*dimer distance of 3.481(5) Å. This second interaction is weak due to the long distance and the inefficient overlap of the radicals. A second type of $TCNQF_4$ radical is present that exhibits only weak interactions with nearest neighbors, with the closest atom contact being a C–N interaction of 3.327(9) Å (Figs. 10d and 10e); the distance of the least squares planes is 2.265(9) Å. Magnetic susceptibility studies of **4b** reveal a diamagnetic ground state (-3.7×10^{-4} emu CGS/mol compared to -3.2×10^{-4} emu CGS/mol estimated from the Pascal constants (22)) which is a signature of radical dimerization. Nevertheless, in this case, Fig. 11 shows that the excited triplet state ($S=1$) is thermally accessible. A fitting of the experimental data by the Bleaney–Bowers equation reveals that only one-half of the radicals are involved in the population of the triplet state with an energy gap of 158 K (28). The

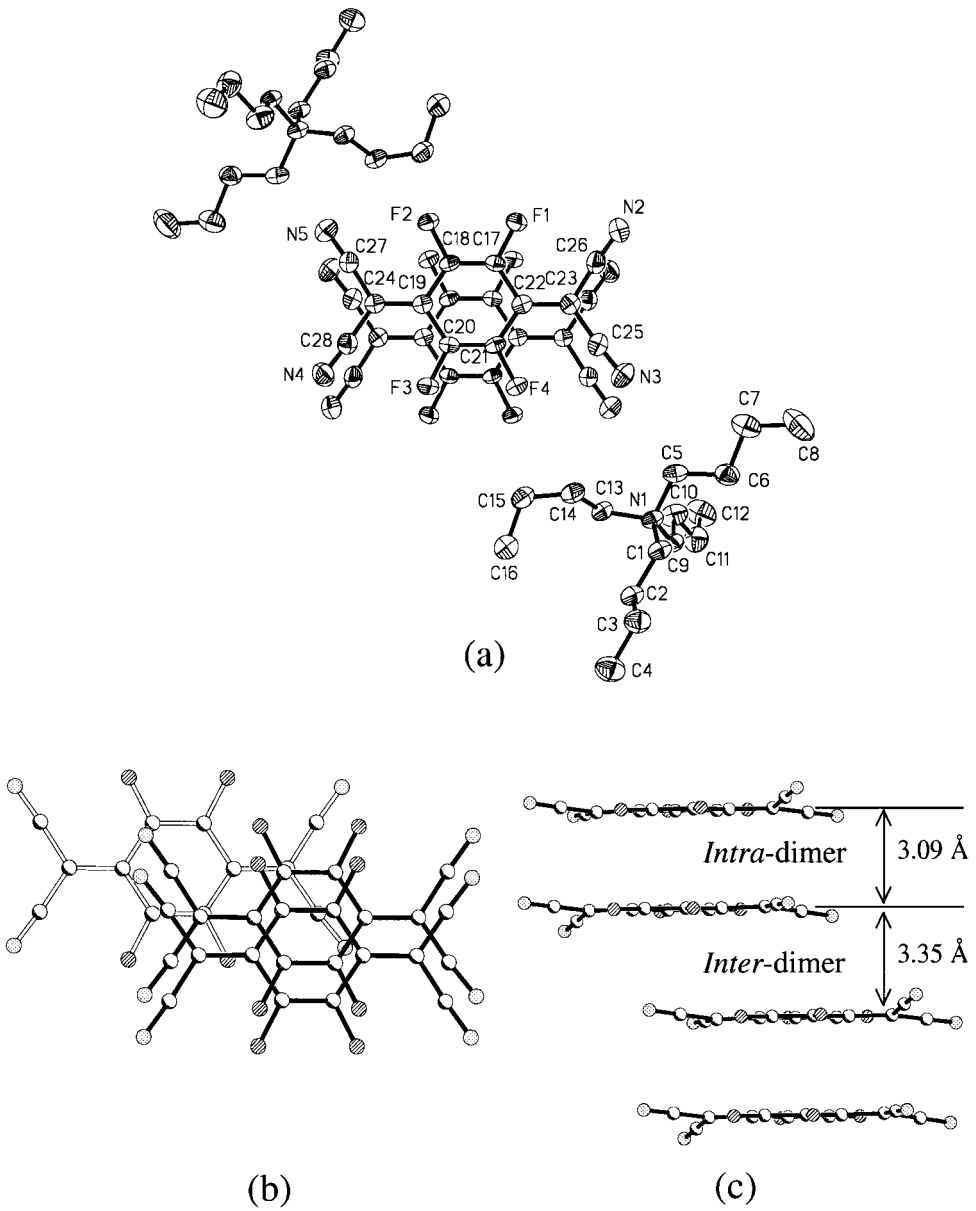

FIG. 9. (a) ORTEP drawing (at the 50% probability level) of the $[n\text{-}Bu_4N][TCNQF_4]$ (**4a**). (b) Top and (c) side view of the stacking motif in $[n\text{-}Bu_4N][TCNQF_4]$ (**4a**).

lack of quantitative Curie law at low temperature indicates that one-half of the $TCNQF_4$ radicals (Figs. 10b and 10c) are completely diamagnetic due to strong dimerization. The remaining radicals (Figs. 10d and 10e) are solely responsible for the observed magnetic behavior.

(iv) Structural analysis of Ag(TCNQF$_4$). The $Ag(TCNQF_4)$ structure is not isostructural to either phase of Ag(TCNQ). A pseudotetrahedral geometry (Fig. 12) is invoked about the silver atoms due to the fourfold coordination of the $TCNQF_4^-$ ligands. This geometry is reminiscent of the motif found in Ag(TCNQ) phase II (7) (Fig. 13) and $Cs_2(TCNQ)_3$ (13a), but is unlike the environment of the Na^+ (13c), K^+ (13f), or Rb^+ (13b) ions in the alkali metal family salts of $TCNQ^-$. $Ag(TCNQF_4)$ is distinct in that adjacent $TCNQF_4^-$ stacks are not rotated 90° with respect to each other, which is a common feature in binary metal/TCNQ salts (7, 13). Instead the twofold rotation axis generates propagated layers of parallel $TCNQF_4$ anions which form columnated stacks along the *b* axis (Fig. 12c). The empty space afforded by one polymeric framework is sufficiently large that a second interpenetrating network is formed as

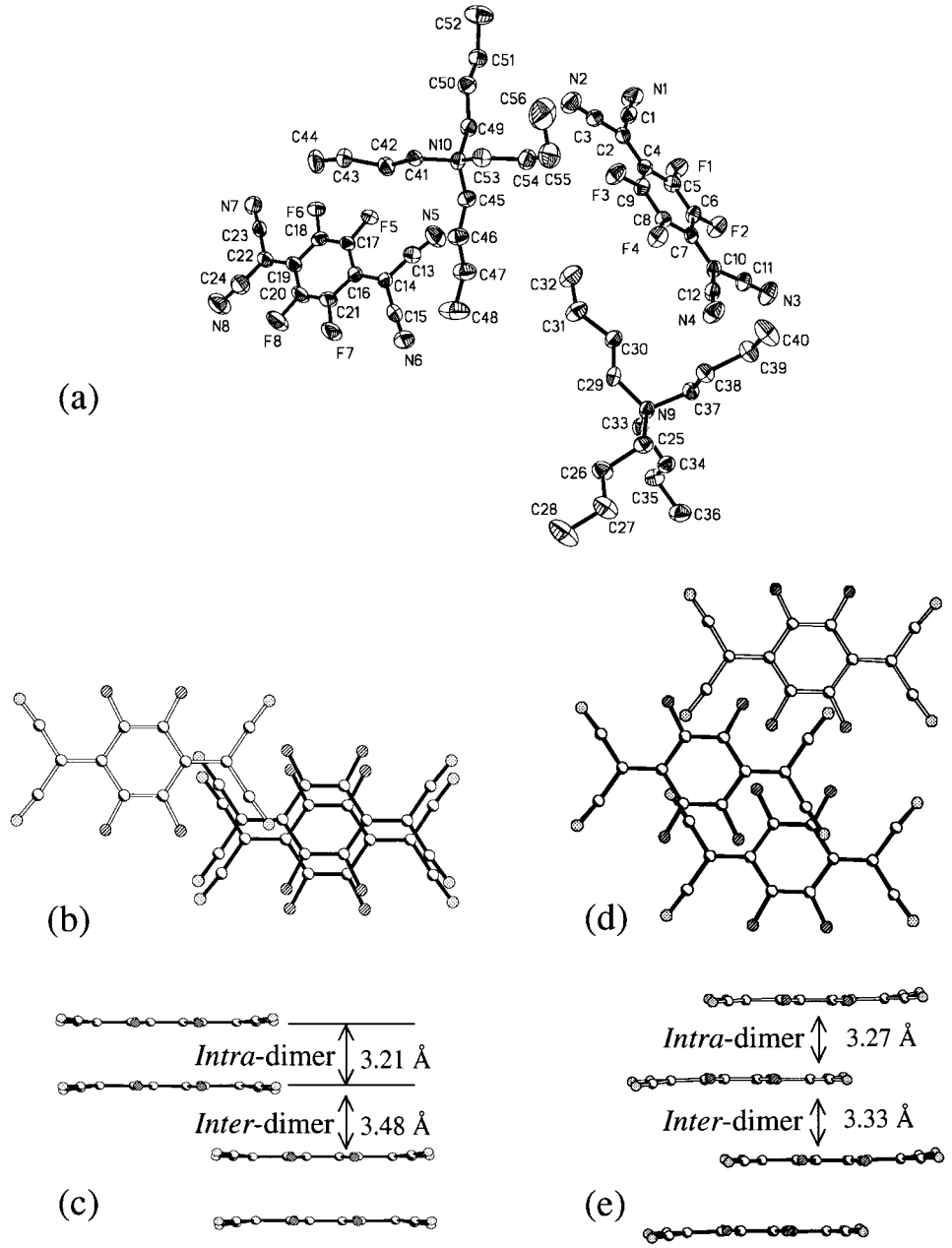

FIG. 10. (a) ORTEP drawing (at the 50% probability level) of [*n*-Bu_4N][$TCNQF_4$] (**4b**). (b), (d) Top and (c), (e) side views of the stacking motifs in [*n*-Bu_4N][$TCNQF_4$] (**4b**).

well (Fig. 12b). The N–Ag–N angles in the range 97.84° to 130.96° are indicative of a highly distorted geometry. In Fig. 12c it is evident that the $TCNQF_4$ anions are nearly perfectly eclipsed, which results in a high degree of dimerization. There are two types of ring-edge dimer interactions at distances of 3.119(2) and 3.330(2) Å, both of which are much shorter then the van der Waals distance of 3.4 Å for carbon atoms. A close structural analogy to Ag($TCNQF_4$) is $Mn(TCNQ)_2(H_2O)_2$ (29), which also contains a ring–edge stacking motif; in this case there is a short intralayer stacking distance of 3.048(2) Å and a longer interlayer interaction distance of ~3.3 Å. There is a difference, however, between $Mn(TCNQ)_2(H_2O)_2$ and Ag($TCNQF_4$) in that the dimer pairs between layers in the Mn compound are rotated by 90°, while the Ag compound exhibits parallel dimer pairs.

As mentioned above, Ag($TCNQF_4$) contains parallel TCNQ stacks unlike the stacks in *M*(TCNQ) (*M* = alkali

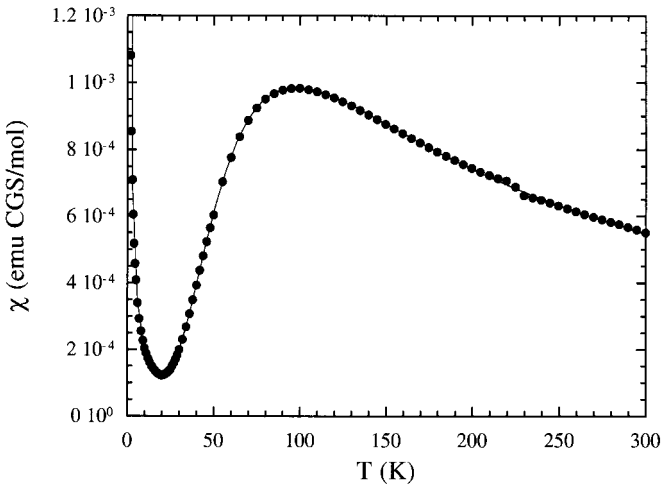

FIG. 11. Temperature dependence of the magnetic susceptibility of [*n*-Bu_4N][$TCNQF_4$] (**4b**). The solid line is the best fitting obtained by the Bleaney–Bowers equation (28).

metals, Ag) which are rotated by 90°. The closest analog of Ag($TCNQF_4$) is Cu(TCNQ) phase II, in which the neighboring TCNQ stacks are also rotated by ~90°; both structures have interpenetrating TCNQ networks. The distances between the centroids of TCNQ anions in the same network is 7.556 Å in compound Ag($TCNQF_4$) versus 7.541 Å in Cu(TCNQ) phase II. The distances between the centroids of TCNQ anions between the two interpenetrating networks is 3.673 Å in Ag($TCNQF_4$) versus 5.331 Å in Cu(TCNQ) phase II. The longer metal nitrile bond lengths in the Ag compound (Ag–N 2.31Å versus Cu–N 1.96 Å) and the more flexible metal nitrile bond angles (N–Ag–N 97.8–131.0° versus N–Cu–N 102.8–114.9°) lead to a more efficient stacking between the two interpenetrating networks in Ag($TCNQF_4$). Of course the greater tendency for $TCNQF_4$ radicals to form dimer stacks could also be contributing significantly to the stabilization of a more closely packed networks.

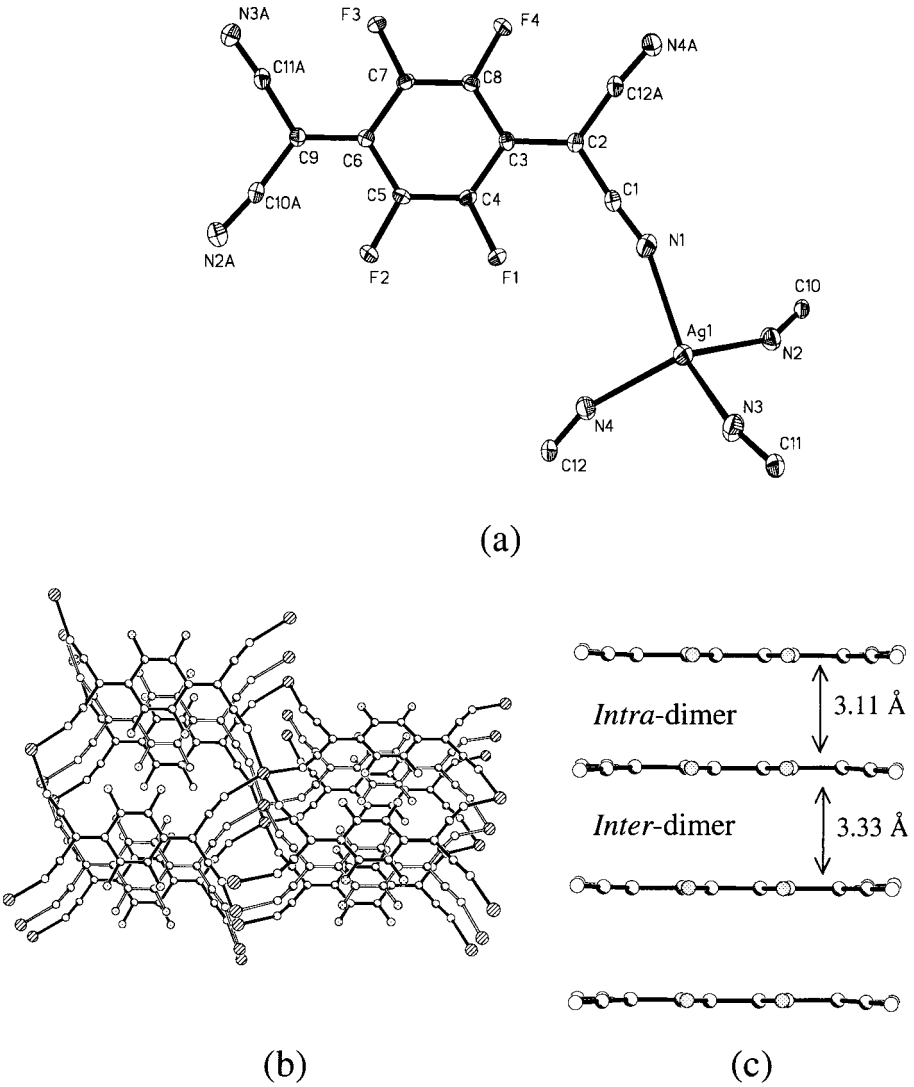

FIG. 12. (a) ORTEP drawing (at the 50% probability level) of Ag($TCNQF_4$) (**5**). (b) Top and (c) side views of the stacking motif.

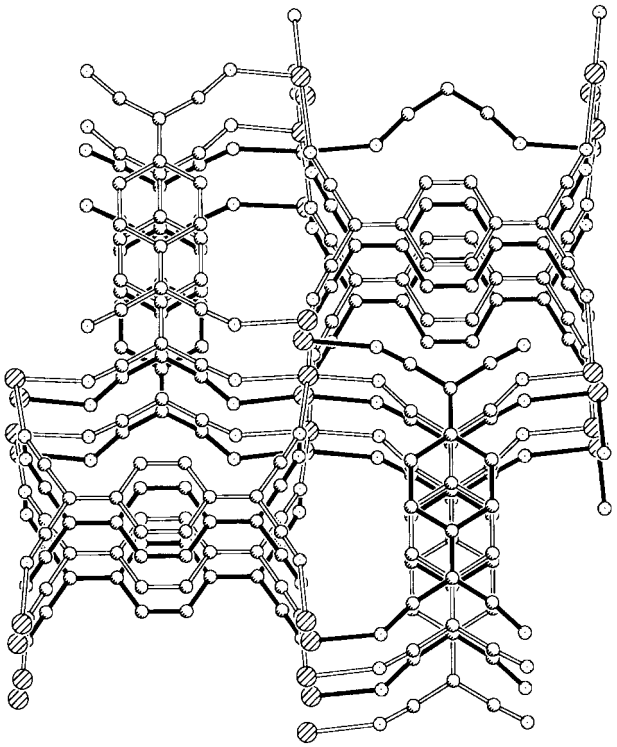

FIG. 13. Packing diagram of the Ag(TCNQ) phase II (**2**) from reference (7).

According to the solid state structure, which indicates a strong dimerization of the $TCNQF_4^-$ radicals, magnetic susceptibility measurements (Fig. 14) reveal essentially diamagnetic behavior with a temperature independent paramagnetism (t.i.p. $= 0.9 \times 10^{-3}$ emu CGS/mol). Similar behavior was observed for Ag(TCNQ) polymorphs which also exhibit t.i.p. between 1.9×10^{-3} (phase II) and 1.4×10^{-3} emu CGS/mol (phase I). A small Curie contribution at low temperature is a signature of defects (or impurities) in the samples (Table 2). In all these silver compounds, the strongly dimerized nature of the organic acceptor is such that the thermal population of the triplet state cannot be observed in the accessible temperature range.

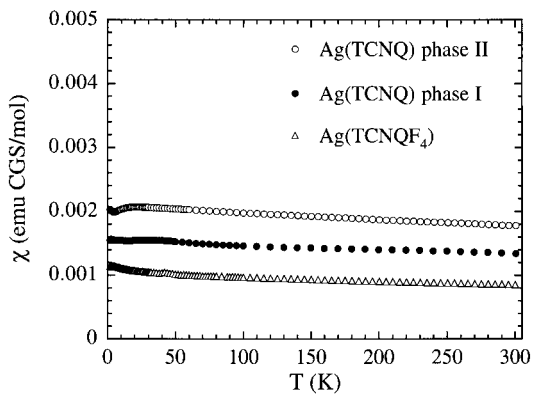

FIG. 14. Temperature dependence of the magnetic susceptibility for Ag(TCNQ) phase I (**1**), phase II (**2**) and Ag(TCNQF$_4$) (**5**).

CONCLUSIONS

One of the outcomes of the present work is the discovery of a previously unrecognized phase of Ag(TCNQ), a material that has been studied as a bistable switching device. Both phases can be synthesized in bulk using two separate synthetic methods, which distinguishes them from the two polymorphs of Cu(TCNQ) which are related by a direct kinetic/thermodynamic relationship. A bulk sample of Ag(TCNQ) phase II prepared from Ag powder and TCNQ is identical to the electrochemically prepared crystal by Shields as verified by X-ray powder diffraction. Ag(TCNQ) phase I does not easily convert to phase II, unlike the two phases of Cu(TCNQ). In the presence of heat and/or light it is possible to observe some conversion of Ag(TCNQ) phase I to phase II, but it is unlikely that a direct conversion of soluble Ag^+ ions and $TCNQ^-$ is occurring as judged by the concomitant formation of Ag metal. In addition to the TCNQ chemistry, our foray into the corresponding reactivity of the much more electron-withdrawing acceptor $TCNQF_4$ has allowed for an expansion of the structural database for these materials. The structure of Ag(TCNQF$_4$) is the first of its kind with a metal bound to $TCNQF_4^-$; the stacking interactions in the $TCNQF_4^-$ derivatives are exceedingly short and are undoubtedly related to the electron withdrawing fluorine groups on the π-delocalized ring. A slipped ring-edge stacking is apparent in the structure of [*n*-Bu_4N][$TCNQF_4$], which is also evident in other organic cation TCNQ salts. Syntheses of other metal-based $TCNQF_4$ compounds will be continued in the future, along with a further expansion into the use of other organic acceptors such as the 2,5-dibromo- and 2,5-dimethoxy derivatives of TCNQ.

Supporting information available. Tables of crystal data, atomic coordinates, bonds lengths and angles, and anisotropic thermal parameters for (**3**) (10 pages), (**4a**) (9 pages), (**4b**) (12 pages), and (**5**) (6 pages) are available from the authors.

ACKNOWLEDGMENTS

We gratefully acknowledge the National Science Foundation (NSF CHE-9906583) for support of this project. We also acknowledge the assistance of Dr. Donald Ward for advice on crystallography and Jeremy Harris for his help on the FESEM measurements.

REFERENCES

1. (a) G. B. Gardner, D. Venkataraman, J. S. Moore, and S. Lee, *Nature* **374,** 792 (1995); (b) O. M. Yaghi, G. Li, and H. Li, *Nature* **378,** 703

(1995); (c) O. M. Yaghi and H. Li, *J. Am. Chem. Soc.* **117,** 10401 (1995); (d) D. Venkataraman, G. B. Gardner, S. Lee, and J. S. Moore, *J. Am. Chem. Soc.* **117,** 11601 (1995); (e) J. A. Whiteford, E. M. Rachlin, and P. J. Stang, *Angew. Chem. Int. Ed. Engl.* **35,** 2524 (1996); (f) O. M. Yaghi and H. Li, *J. Am. Chem. Soc.* **118,** 295 (1996); (g) O. M. Yaghi, H. Li, and T. L. Groy, *J. Am. Chem. Soc.* **118,** 9096 (1996); (h) B. Olenyuk, J. A. Whiteford, and P. J. Stang, *J. Am. Chem. Soc.* **118,** 8221 (1996).

2. (a) J. M. Manriquez, G. T. Yee, S. McLean, A. J. Epstein, and J. S. Miller, *Science* **252,** 1415 (1991); (b) H. Tamaki, Z. J. Zhuang, N. Matsumoto, S. Kida, M. Koikawa, N. Achiwa, Y. Hashimoto, and H. Okawa, *J. Am. Chem. Soc.* **114,** 6974 (1992); (c) H. O. Stumpf, Y. Pei, O. Kahn, J. Sletten, and J. P. Renard, *J. Am. Chem. Soc.* **115,** 6738 (1993); (d) K. Inoue and H. J. Iwamura, *J. Am. Chem. Soc.* **116,** 3173 (1994); (e) M. Ohba, N. Maruono, H. Okawa, T. Enoki, and J.-M. Latour, *J. Am. Chem. Soc.* **116,** 11566 (1994). (f) O. Kahn, *in* "Molecular Magnetism: From Molecular Assemblies to the Devices," (E. Coronado, P. Delhaes, D. Gatteschi, and J. S. Miller, Eds.), NATO ASI Series E321, pp. 243–288, Kluwer, Dordrecht, 1996; (g) S. Decurtins, H. W. Schmalle, P. Schneuwly, L.-M. Zheng, J. Ensling, and A. Hauser, *Inorg. Chem.* **34,** 5501 (1995); (h) H. Miyasaka, N. Matsumoto, H. Okawa, N. Re, E. Gallo, and C. Floriani, *Angew. Chem. Int. Ed. Engl.* **34,** 1446 (1995); (i) M. Ohba, H. Okawa, T. Ito, and A. J. Ohto, *J. Am. Chem. Soc. Chem. Commun.* 1545 (1995); (j) C. Michaut, L. Ouahab, P. Bergerat, O. Kahn, and A. Bousseksou, *J. Am. Chem. Soc.* **118,** 3610 (1996). (k) G. de Munno, T. Poerio, G. Viau, M. Julve, F. Lloret, Y. Journaux, and E. Riviere, *Chem. Commun.* 2587 (1996).
3. (a) A. Aumüller, P. Erk, G. Klebe, S. Hünig, J. von Schütz, and H. Werner, *Angew. Chem. Int. Ed. Engl.* **25,** 740 (1986). (b) A. Aumüller, P. Erk, and S. Hünig, *Mol. Cryst. Liq. Cryst.* **156,** 215 (1988). (c) P. Erk, H.-J. Gross, U. L. Hünig, H. Meixner, H.-P. Werner, J. U. von Schütz, and H. C. Wolr, *Angew. Chem. Int. Ed. Engl.* **28,** 1245 (1989). (d) R. Kato, H. Kobayashi, and A. J. Kobayashi, *J. Am. Chem. Soc.* **111,** 5224 (1989); (e) A. Aumüller, P. Erk, S. Hünig, E. Hädicke, K. Peters, and H. G. von Schnering, *Chem. Ber.* **124,** 2001 (1991). (f) K. Sinzger, S. Hünig, M. Jopp, D. Bauer, W. Beitsch, J. U. von Schütz, H. C. Wolf, R. K. Kremer, T. Metzenthin, R. Bau, S. I. Khan, A. Lindbaum, C. L. Lengauer, and E. Tillmanns, *J. Am. Chem. Soc.* **115,** 7696 (1989).
4. See for example (a) P. J. Fagan, M. D. Ward, and J. C. Calabrese, *J. Am. Chem. Soc.* **111,** 1698 (1989); (b) T. Iwamaoto, *in* "Inclusion Compounds: Inorganic and Physical Aspects of Inclusion," (T. Iwamoto, J. L. Atwood, J. E. D. Davies, and D. D. MacNicol, Eds.), Vol. 5, Chap. 6, p. 177, Oxford Univ. Press, Oxford, 1991; (c) R. Robson, B. F. Abrahms, S. R. Batten, R. W. Gable, B. F. Hoskins, and J. Liu, *in* "Supramolecular Architecture" (T. Bein, Ed.), p. 256, American Chemical Society: Washington, DC, 1992; (d) R. Tannenbaum, *Chem. Mater.* **6,** 550 (1994); (e) E. C. Constable, *Prog. Inorg. Chem.* **42,** 67 (1994); (f) J. Lu, W. T. A. Harrison, and A. J. Jacobson, *Angew. Chem. Int. Ed. Engl.* **24,** 2557 (1995). (g) K. R. Dunbar and R. A. Heintz, *Prog. Inorg. Chem.* **35,** 4449 (1996); (i) J. A. Whiteford, E. M. Rachlin, and P. J. Stang, *Angew. Chem. Int. Ed. Engl.* **35,** 2524 (1996); (j) C. V. K. Sharma and M. J. Zaworotko, *Chem. Commun.* 2655 (1996); (k) K. A. Hirsch, S. R. Wilson, and J. S. Moore, *Inorg. Chem.* **36,** 2960 (1997).
5. (a) P. Lacroix, O. Kahn, A. Gliezes, L. Valade, and P. Cassoux, *Nouv. J. Chim.* 643 (1985); (b) R. Gross and W. Kaim *Angew. Chem. Int. Ed. Engl.* **26,** 251 (1987); (c) D. G. Humphrey, G. D. Fallon, and K. S. Murray, *J. Chem. Soc. Chem. Commun.* **20,** 1356 (1988). (d) S. L. Bartley, and K. R. Dunbar, *Angew. Chem. Int. Ed. Engl.* **30,** 448 (1991); (e) L. Ballester, M. Barral, A. Gutiérrez, R. Jiménez-Apararicio, J. Martinez-Muyo, M. Perpiñan, M. Monge, and C. Ruiz-Valero, *J. Chem. Soc. Chem. Commun.* 1396 (1991); (f) J. P. Cornelissen, J. H. van Diemen, L. R. Groeneveld, J. G. Haasnoot, A. L. Spek, and J. Reedijk, *Inorg. Chem.* **31,** 198 (1992); (g) H. Oshio, E. Ino, I. Mogi, and T. Ito, *Inorg. Chem.* **33,** 5697 (1993); (h) L. Ballester, M. Barral, A. Gutiérrez, M. Perpiñan, M. Monge, C. Ruiz-Valero, and A. Sánchez-Pélaez, *Inorg. Chem.* **33,** 2142 (1994); (i) K. R. Dunbar and X. Ouyang, *Mol. Cryst. Liq. Cryst. Sci. Technol.* **273,** 21 (1995); (j) H. Oshio, E. Ino, T. Ito, and Y. Maeda, *Bull. Chem. Soc. Jpn.* **68,** 889 (1995); (k) K. R. Dunbar, *Angew. Chem.* **35,** 1659 (1996); (l) S. Decurtins, K. R. Dunbar, C. J. Gomez-Garcia, T. Mallah, R. G. Raptis, D. Talham, and J. Veciana, *in* "Molecular Magnetism: From Molecular Assemblies to the Devices," (E. Coronado, P. Delhaès, D. Gatteschi, and J. S. Miller, Eds.), NATO ASI Series E321, Kluwer, Dordrecht, 1996; (m) K. R. Dunbar and X. Ouyang, *Chem. Commun.* 2427 (1996); (n) H. Zhao, R. A. Heintz, R. D. Rogers, and K. R. Dunbar, *J. Am. Chem. Soc.* **118,** 12844 (1996); (o) K. R. Dunbar and X. Ouyang, *Inorg. Chem.* **35,** 7188 (1996); (p) M. T. Azcondo, C. J. Ballester, A. Gutiérrez, M. Perpiñan, U. Amador, C. Ruiz-Valero, and C. Bellitto,. *J. Chem. Soc. Dalton Trans.* 3015 (1996).
6. For an excellent review on the subject of σ coordination to TCNX molecules, see W. Kaim and M. Moscherosch, *Coord. Chem. Rev.* **129,** 157 (1994).
7. Structure of Ag(TCNQ) phase II: Shields, L. *J. Chem. Soc. Faraday Trans. 2* **81,** 1 (1985).
8. (a) R. S. Potember, T. O. Poehler, and D. O. Cowan, *Appl. Phys. Lett.* **34,** 405 (1979). (b) R. S. Potember, T. O. Poehler, A. Rappa, D. O. Cowan, and A. N. Bloch, *J. Am. Chem. Soc.* **102,** 3659 (1980). (c) R. S. Potember, T. O. Poehler, D. O. Cowan, P. Brant, F. L. Carter, and A. N. Bloch, *Chem. Scr.* **17,** 219 (1981); (d) E. I. Kamistos and W. M. Risen, Jr., *Solid State Commun.* **42,** 561 (1982); (e) R. S. Potember, T. O. Poehler, D. O. Cowan, F. L. Carter, and P. I. Brant, *in* Molecular Electronic Devices (F. L. Carter, Ed.), p. 73, Dekker, New York, 1982; (f) R. S. Potember, T. O. Poehler, and R. C. Benson, *Appl. Phys. Lett.* **41,** 548 (1982). (g) R. S. Potember, T. O. Poehler, A. Rappa, D. O. Cowen, and A. N. Bloch, *Synth. Met.* **4,** 371 (1982). (h) E. I. Kamitsos and W. M. Risen, *Solid State Commun.* **45,** 165 (1983). (i) E. I. Kamitsos and W. M. Risen, *J. Chem. Phys.* **79,** 477 (1983); (j) E. I. Kamitsos and W. M. Risen, Jr. *J. Chem. Phys.* **79,** 5808 (1983). (k) R. C. Benson, R. C. Hoffman, R. S. Potember, E. Bourkoff, and T. O. Poehler, *Appl. Phys. Lett.* **41,** 548 (1983). (l) T. O. Poehler, R. S. Potember, R. Hoffman, R. C. Benson, *Mol. Cryst. Liq. Cryst.* **107,** 91 (1984). (m) E. I. Kamistos, and W. M. Risen, Jr., *Mol. Cryst. Liq. Cryst.* **134,** 31 (1986); (n) R. S. Potember, T. O. Poehler, R. C. Hoffman, K. R. Speck, and R. C. Benson, *in* "Molecular Electronic Devices II" (F. L. Carter, Ed.), p. 91, Dekker, New York, 1987; (o) S. Wakida and Y. Ujihira, *J. Appl. Phys.* **27,** 1314 (1988). (p) R. C. Hoffman and R. S. Potember, *Appl. Opt.* **28**(7), 1417 (1989); (q) H. Duan, M. D. Mays, D. O. Cowan, and J. Kruger, *Synth. Met.* **28,** C675 (1989); (r) C. Sato, S. Wakamatsu, K. Tadokoro, and K. Ishii, *J. Appl. Phys.* **68**(12), 6535 (1990); (s) S. Yamaguchi, C. A. Viands and R. S. Potember, *J. Vac. Sci. Technol.* **9,** 1129 (1991); (t) Z. Y. Hua and G. R. Chen, *Vacuum* **43,** 1019 (1992); (u) J. J. Hoagland, X. D. Wang and K. W. Hipps, *Chem. Mater.* **5,** 54 (1993); (v) S. G. Liu, Y. Q. Liu, P. J. Wu, and D. B. Zhu,. *Chem. Mater.* **8,** 2779 (1996). (w) S. G. Liu, Y. Q. Liu, and D. B. Zhu, *Thin Solid Films* **280,** 271. (1996); (x) S. Q. Sun, P. J. Wu, and D. B. Zhu, *Solid State Commun.* **99,** 237 (1996); (y) S. G. Liu, Y. Q. Liu, P. J. Wu, D. B. Zhu, H. Tian, and K. C. Chen, *Thin Solid Films* **289,** 300 (1996).
9. R. A. Heintz, H. Zhao, X. Ouyang, G. Grandinetti, J. Cowen, and K. R. Dunbar, *Inorg. Chem.* **38,** 144 (1999).
10. (a) T. J. Emge, W. A. Bryden, F. M. Wiygul, D. O. Cowan, and T. J. Kistenmacher, *J. Chem. Phys.* **77,** 3188 (1982). (b) R. A. Metzger, N. E. Heimer, D. Gundel, H. Sixi, R. H. Harms, H. J. Keller, D. Nöthe, and D. Wehe, *J. Chem. Phys.* **77,** 6203 (1982); (c) F. M. Wiygul, T. J. Emge, and T. J. Kistenmacher, *Mol. Cryst. Liq. Cryst.* **90,** 163 (1982). (d) T. J. Emge, D. O. Cowan, A. N. Bloch, and T. J. Kistenmacher, *Mol. Cryst. Liq. Cryst.* **95,** 191 (1983).
11. (a) M. T. Jones, T. Maruo, S. Jansen, J. Roble, and R. D. Rataiczak, *Mol. Cryst. Liq. Cryst.* **134,** 21 (1986). (b) T. Maruo, R. D. Rataiczak, and M. T. Jones, *Mol. Phys.* **73,** 1365 (1991); (c) T. Sugano, T. Fukasawa, and M. Kinoshita, *Synth. Met.* **41,** 3281 (1991); (d) G.

Agostini, C. Corvaja, G. Giacometti, and L. Pasimeni, *Chem. Phys.* **173,** 177 (1993); (e) T. Otsubo, Y. Kono, N. Hozo, H. Miyamoto, Y. Aso, F. Ogura, T. Tanaka, and M. Sawada, *Bull. Chem. Soc. Jpn.* **66,** 2033 (1993); (f) H. Nishikawa, K. Kawakami, H. Fujiwara, T. Uehara, Y. Misaki, and T. Yamabe, *Synth. Met.* **56,** 1983 (1993); (g) Y. Nakamura, H. Iwamura, *Bull. Chem. Soc. Jpn.* **66,** 3724 (1993); (h) T. Sugimoto, M. Tsujii, E. Murahashi, H. Makatsuji, J. Yamauchi, H. Fujita, Y. Kai, and N. Hosoito, *Mol. Cryst. Liq. Cryst.* **232,** 117 (1993).

12. (a) M. Meneghetti, A. Girlando, and C. Pecile, *J. Chem. Phys.* **83,** 3134 (1985); (b) M. Meneghetti, and C. Pecile, *J. Chem. Phys.* **84,** 4149 (1986). (c) M. Meneghetti, R. Bozio, and C. Pecile, *Synth. Met.* **19,** 451 (1987). (d) M. Meneghetti and R. Bozio, *J. Chem. Phys.* **89,** 2704 (1988).
13. (a) C. J. Fritchie, Jr. and P. Arthur, *Acta Crystallogr.* **21,** 139 (1966); (b) A. Hoekstra, T. Spoelder, and A. Vos, *Acta Crystallogr. B* **28,** 14 (1972); (c) M. Konno, Y. Saito, *Acta Crystallogr. B* **30,** 1294 (1979); (d) M. Murakami and S. Yoshimura, *Bull. Chem. Soc. Jpn.* **48,** 157 (1975); (e) M. Konno and Y. Saito, *Acta Crystallogr. B* **31,** 2007 (1975); (f) M. Konno, T. Ishii, and Y. Saito, *Acta Crystallogr. B* **33,** 763 (1977); (g) H. Endres, *in* "Extended Linear Chain Compounds" (J. S. Miller, Ed), Vol. 3, p. 263, Plenium, New York, 1983.
14. L. R. Melby, R. J. Harder, W. R. Hertler, W. Mahler, R. E. Benson, and W. E. Mochel, *J. Am. Chem. Soc.* **84,** 3374 (1962).
15. (a) R. C. Wheland and E. L. Martin, *J. Org. Chem.* **40**(21), 3101 (1975). (b) M. Meneghetti, R. Bozio, C. Bellitto, and C. Pecile, *J. Chem. Phys.* **89**(5), 2704 (1988); (c) M. S. Khatkale and J. P. Devlin, *J. Chem. Phys.* **70**(04), 1851 (1979).
16. SMART 1000, Brucker Analytical X-Ray Instruments, Madison, WI 53719, 1999.
17. SAINT 1000, Brucker Analytical X-Ray Instruments, Madison, WI 53719, 1999.
18. G. M. Sheldrick, "SADABS, Siemens Area Detector Absorption (and other) Correction," Univ. of Göttinger, Göttinger, Germany, 1998.
19. SHELXTL ver. 5.10, Reference Manual, Bruker Industrial Automation, Analytical Instrument, Madison, WI 53719, 1999.
20. G. M. Sheldrick, "SHELXS, Program for the Solution of Crystal Structure," Release 97-2, Univ. of Göttinger, Göttinger, Germany, 1997.
21. G. M. Sheldrick, "SHELX97, Program for Refinement of Crystal Structure," Release 97-2, Univ. of Göttinger, Göttinger, Germany, 1997.
22. E. A. Boudreaux, and J. N. Mulay, "Theory and Applications of Molecular Paramagnetism," Wiley, New York, 1976.
23. (a) B. Lunille, and C. Pecile, C. *J. Chem. Phys.* **52,** 2375 1970; (b) R. Bozio, A. Girlando, and C. Pecile, *J. Chem. Soc., Faraday Trans.* **2 71,** 1237 (1975); (c) R. P. Van Duyne, M. R. Suchanski, J. M. Lakovits, A. R. Siedle, K. D. Parks, and T. M. Cotton, *J. Am. Chem. Soc.* **101,** 2832 (1979); (d) J. S. Chappell, A. N. Bloch, A. Bryden, M. Maxfiled, T. O. Poehler, and D. O. Cowan, *J. Am. Chem. Soc.* **103,** 2442 (1981); (e) J. P. Farges, A. Brau, and P. Dupuis, *Solid State Commun.* **54**(6), 531 1985; (f) M. Inoue and M. B. Inoue, *J. Chem. Soc. Faraday Trans. 2* **81,** 539 (1985); (g) M. Inoue and M. B. Inoue, *Inorg. Chem.* **25,** 37 (1987); (h) M. Inoue, M. B. Inoue, Q. Fernando, and K. W. Nebesny, *J. Phys. Chem.* **91,** 527 (1987). (i) W. Pukaki, M. Pawlak, A. Graja, M. Lequan, and R. M. Lequan, *Inorg. Chem.* **26,** 1328 (1987).
24. (a) M. Meneghetti and C. Pecile, *J. Chem. Phys.* **84**(8), 4149 (1986); (b) M. Meneghetti, R. Bozio, and C. Pecile, *Synth. Met.* **19,** 451 (1987); (c) M. Meneghetti and R. Bozio, *J. Chem. Phys.* **5,** 2704 (1988); (d) L. Y. Chiang and D. P. Goshorn, *Mol. Cryst. Liq. Cryst.* **26,** 229 (1989).
25. (a) Y. Yashihiro, Y. Furukawa, A. Kobayashi, M. Tasumi, R. Kato, and H. Kobayashi, *J. Chem. Phys.* **100,** 2449 (1994). (b) A. Kobayashi, R. Kato, H. Kobayashi, T. Mori, and H. Inokuchi, *Solid State Commun.* **64,** 45 (1987). (c) R. D. Willett and G. Long, pers. commun.
26. P. E. Werner, *J. Appl. Cryst.* **18,** 367 (1985); TREOR program was adapted to PC and PROSZKI system at Jaqielloniam University 1989.
27. (a) H. Kobayashi, T. Danno, and Y. Saito, *Acta Crystallogr. B* **29,** 2693 (1973); (b) H. Kobayashi, *Acta. Crystallogr. B* **34,** 2818 (1978); (c) A. Fihol, M. Rovira, C. Hauw, J. Gaultier, D. Chasseau, and P. Dupuis, *Acta Crystallogr. B* **35,** 1652 (1979); (d) R. P. Shibaeva, V. F. Kaminskii, and M. A. Simonov, *Cryst. Struct. Commun.* **9,** 655 (1980).
28. We fit our experimental data using the Bleaney–Bowers formula and a Curie law for $S = 1/2$, equation 1 where N is the number of $TCNQF_4^-$ coupled into dimers, N' is the number of molecules with an unpaired spin, μ_B is the Bohr magneton, and the g-factor is assumed to be equal to 2 (usual for TCNQ compounds):

$$\chi_p = \frac{2Ng^2\mu_B^2}{kT}\left(\frac{1}{3+\exp[-2J/(kT)]}\right) + \left(\frac{N'g^2\mu_B^2}{4kT}\right)$$

29. H. Zhao, R. A. Heintz, X. Ouyang, and K. R. Dunbar, *Chem. Mater.* **11,** 736 (1999).